Land surface evapo-transpiration for water balance in the Kirindi Oya watershed. A remote sensing approach.

Eng. Palitha Bandara*, Dr. Wim Bastiaanssen**/***, Dr. Lucas Janssen**

* Irrigation Department, P.O. Box 1138, Colombo, Sri Lanka.
** International Institute for Aerospace Survey and Earth science (ITC), P.O.Box 6, 7500 AA, Enschede, The Netherlands.
*** International Irrigation Management Institute, P.O.Box 2075, Colombo, Sri Lanka.

Abstract

The world has entered a new era of water management that requires large increases in the productivity of water use, in addition to water development programs. The management of irrigated areas is becoming more critical by increasing demands for food and water. The Kirindi Oya watershed in Southeast Sri Lanka needs improvements for the utilisation of land and water resources.
The Kirindi Oya watershed exhibits many different small-scale agro-ecosystems. The water consumption of these systems is difficulty to measure. Water "wasted" or "discharged" on one part of the watershed is often recaptured and re-used in another part. Hence, improvements in water use efficiency would generate large amounts of additional water supply. The wide diversity in vegetation and hydrology can be surveyed with remote sensing. Satellite images acquired from the Landsat Thematic Mapper have been used for this research.
An evapo-transpiration algorithm based on the surface energy balance (SEBAL) has been applied to determine the actual evapo-transpiration during the different moments of the year. SEBAL computes the actual evapo-transpiration on pixel by pixel basis, independent from the type of the land cover / land use.
SEBAL computes the *actual evapo-transpiration* of different land use /land cover classes. Conventional methods compute the *potential evapo-transpiration* of selected agricultural crop types with respect to a reference crop.
Actual evapo-transpiration of different land use/ land cover samples of the Kirindi Oya watershed has been computed on pixel basis. The results are shown in graphical form.
It is concluded that advance remote sensing techniques can provide basic data for proper land use planning for the water management at the watershed level.

Key words: Atmospheric correction, Evapo-transpiration, Heat flux, Radiation, Spectral range, Surface albedo, Surface energy, Surface temperature, Vegetation index.

1. Introduction

1.1 Water use of the Kirindi Oya watershed

The water, which inflows to the Kirindi oya watershed, re-cycles among its land cover classes. At present there is no precisely developed system for the computation of optimum utilisation of water used in different land cover classes. Since wastewater from one land cover class within the watershed area is re-used by another land cover class, optimal water utilisation systems cannot be planned, focusing on one particular issue.

With the land development programs and increase of population, water availability becomes a primary and scare resource. In order to manage such a scare resource, water development strategies are needed. Hence, planning for optimal water utilisation systems with effective and efficient water management strategy is necessary. Water consumption varies on land cover class, land use type, and the seasonal changes. Hence, ***it is required to know the water consumption of different land cover classes and land use types for water use planning.*** Integrated water management system for the whole watershed area is therefore needed.

1.2 Actual water consumption and Evapo-transpiration [ET]

Actual water consumption for a particular land cover class can be described in terms of actual plant water requirement and the surface water evaporation, of that class subject to seasonal changes. This is related to the term evapo-transpiration (ET), which is one of the key parameters of the water balance. Evapo-transpiration can be defined as the net water loss from the earth surface characterised by a combination of evaporation and transpiration. Evaporation

represents a significant mass and energy transfer from the ground to the atmosphere. Transpiration refers to water loss from plants into the atmosphere through stomata opening. Computation of actual evapo-transpiration for a particular land cover class during a time period relates the actual water consumption of that land cover class for that specific time period. This information is required for the planning of integrated water management strategy at the watershed level.

1.3 A remote sensing approach

Methods have been developed for the computation of actual evapo-transpiration values for land cover class by using space borne remotely sensed data. It has to be investigated how these methods could be applied for the Kirindi Oya watershed. Remote sensing measurements of land surface radiative properties offer a means to indirectly measure land surface state conditions on a range scale. A Surface Energy Balance Algorithm for Land (SEBAL) has been developed to convert these state conditions into surface flux densities. Although the concept has a physical basis, the parameters are estimated by empirical relationships (Bastiaanssen, 1995).

It is impossible to measure the water balance terms with remote sensing techniques. But, remote sensing techniques could be used to compute actual evapo-transpiration, which is one of the terms of water balance. The actual, potential and relative evapo-transpiration is linked to the terms of the surface energy balance, which can be detected with remote sensing techniques. This is the basic relationship between the SEBAL and the water balance. SEBAL has been developed to solve the equation for surface energy balance on pixel by pixel basis .The main advantage of this method is that it does not need land use data for ET calculation.

2. Material and the SEBAL model

2.1 Space borne remotely sensed data

Space borne remotely sensed data, the data about spectral radiance, is required for the land cover classification and for the SEBAL. The SEBAL process requires spectral data of thermal infrared range. Landsat Thematic Mapper (Landsat TM) records seven spectral bands with longest wavelength in band 6, the thermal infrared band. Other bands represent the visible and infrared ranges. A Landsat TM data set acquired on 19th June 1995 is used for the sample study.

2.2 Topographic , land use and meteorological data

i. The topo-maps for co-ordinate transferring (georeferencing)
ii. Up to date land use maps are required to identify the present land cover / land use of the area concern.
iii. Air temperature data – Maximum and minimum Temperature data, for the date of satellite data captured. These data are required for the atmospheric correction of the spectral thermal radiation.
iv. Relative humidity – The data is required to calculate the moist air density in the SEBAL.

2.3 SEBAL model

Application of the Surface energy balance algorithm for land (SEBAL) for the computation of the actual evapo-transpiration of the study area is the next part. The SEBAL model is based on the surface energy balance of the land surface, which can be described as follows (Bastiaanssen, 1995);

$$Q^* = G_0 + H + \lambda E \quad [W\,m^{-2}] \qquad (1)$$

Where

Q^* = net radiation absorbed at the land surface	$[Wm^{-2}]$
G_0 = soil heat flux to warm or cool the soil	$[Wm^{-2}]$
H = sensible heat flux to warm the atmosphere	$[Wm^{-2}]$
λE = latent heat flux associated to the actual evaporation of water	$[Wm^{-2}]$

Using the TM data sets, latent heat flux (λE) density of the surface energy balance, can be computed on pixel-by-pixel basis through the SEBAL. Evaporative fraction (Λ) can also be calculated from the SEBAL. Using additional input parameters with the SEBAL outputs, actual evapo-transpiration map can be computed on pixel-by-pixel basis. The model for SEBAL is shown in the Fig.1.

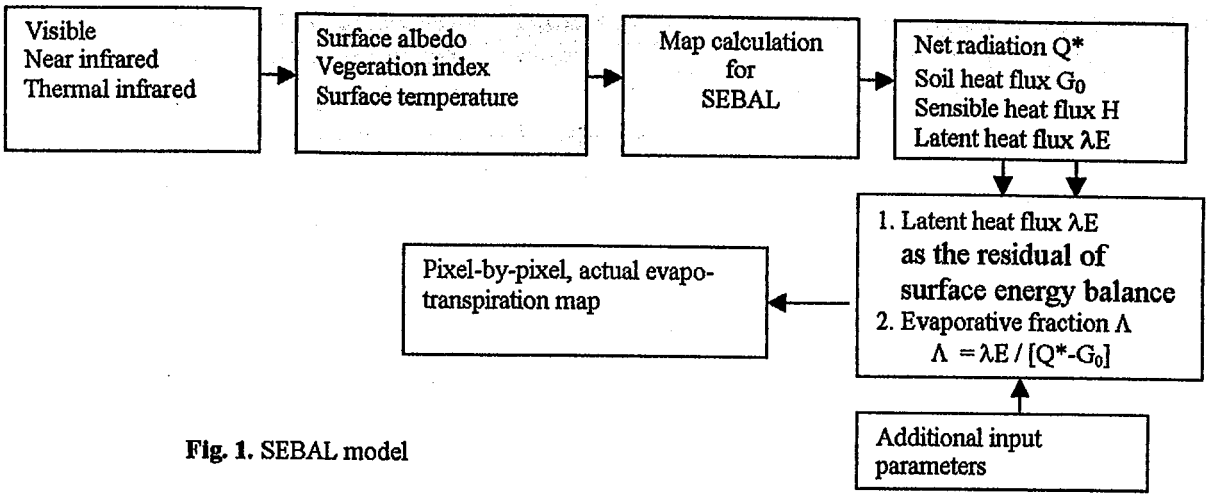

Fig. 1. SEBAL model

3. General physics of SEBAL

3.1 Surface energy balance

The surface of the earth is continually reflecting, absorbing, and emitting energy. The principle source of energy at the earth's surface is radiant energy from the sun. At any time, the balance achieved between energy received, energy stored, and energy lost from a given portion of the earth's surface represents an energy budget for that portion of the earth. The particular energy budget achieved depends upon the energy supply, characteristics of the surface, and influence of the hydrologic cycle. The land cover, i.e. soil, water, and vegetation, influences operation of hydrologic cycle (Reeves, 1975).

3.2 Net radiation flux density (Q*)

Emissivity (ε_0) indicates the ratio of the radiant energy of a certain wavelength at a certain temperature and the radiant energy of a black body of the same wavelength and at the same. The sun emits radiation as a black body ($\varepsilon_0 = 1$). The emission of solar energy is exclusively dependent on the temperature of the body and its surface emissivity (Reeves, 1975).
The principal energy source that drives the land surface flux densities G_0, H, and λE, is delivered by net radiation flux density Q*. For a flat horizontal and homogeneous surface, the integrated wavelength electromagnetic balance in terms of the up (↑) and downwelling (↓) radiative propagation is related to Q* as follows (Basteaanssen, 1995);

$$Q^* = K^{\downarrow} - K^{\uparrow} + L^{\downarrow} - L^{\uparrow} \qquad [Wm^{-2}] \qquad (2)$$

Where K represents the shortwave (0.3 – 3 μm) and L the longwave (3 to 100 μm) radiation components. When electromagnetic radiation strikes an object, different interactions such as transmission, absorption, scattering and emission between radiation and objects arise. The spectrally emitted radiances, which are related to temperature, are calculated through Plank's law for emission, which is valid for black bodies (Reeves, 1975). On contrary, grey body radiators reflect a small fraction of long wave radiation ($\varepsilon_0 \neq 1$). Natural land surfaces behave usually as grey bodies and consequently a correction is required to interpret spectral radiance measurements into temperature.

The net radiation is converted at earth's surface into the sum of land surface flux densities and which is called the surface energy balance (Eq. 1).

3.3 Soil heat flux density (G_0) and sensible heat flux density (H)

The signs of the energy balance components are dependent on time of day and climatic conditions. During the day, the soil and the crop absorb the radiation from the sun. Thus, the soil and canopy surfaces are warmer than the air so that sensible heat flux, H, is away from the crop volume. During the day, the soil surface is warmer than the soil at greater depths so that soil heat flux, G_0, is downwelling (↓) from the crop volume. At night, soil and canopy surfaces lose heat through the emission of longwave radiation because longwave radiation emitted from the crop volume is nearly always greater than atmospheric counter radiation. Since heat deficit cannot be made up by radiation from the sun, soil heat flux

and sensible heat flux are toward the crop volume to counteract the radiation loss. But, conditions may exit where the air is cooler than the canopy and soil surfaces during the night. In such a case, sensible heat flux will be away from the crop volume during the night (Reeves, 1975).

3.4 Latent heat flux density (λE)

During the day latent heat flux is away from the crop volume. At night latent heat flux may be away or toward the crop volume depending on the respective temperatures of the air and crop and soil surfaces. In dry climatic conditions, latent heat flux will continue to be away from the crop volume both day and night, and dew formation will not occur. Horizontal divergence terms will normally be greater than the day due to the higher wind speed. Divergence may be influence at night if movement of frontal system occurs. Over large macro-climatic land areas, horizontal divergence of latent heat must be included because of the large amount of water vapour present in the air (Reeves, 1975).

3.5 Difference between net radiation and soil heat flux density ($Q^* - G_0$)

The difference between net radiation and soil heat flux ($Q^* - G_0$) determines the available energy to be portioned between the surrounding environment and the heat required for evaporation. When water is available for evapo-transpiration and if atmospheric water pressure is low, then most of the energy will be used to evaporate water (latent heat flux). Conversely, if moisture is limited, then the available energy, which could have been used for evapo-transpiration, is now made available for sensible heat flux (Reeves, 1975).

3.6 Sensible heat flux density and assignment of dry pixels

Typical polynomial regression reality between the surface temperature and the surface albedo (r_0) is shown in the Fig 2.

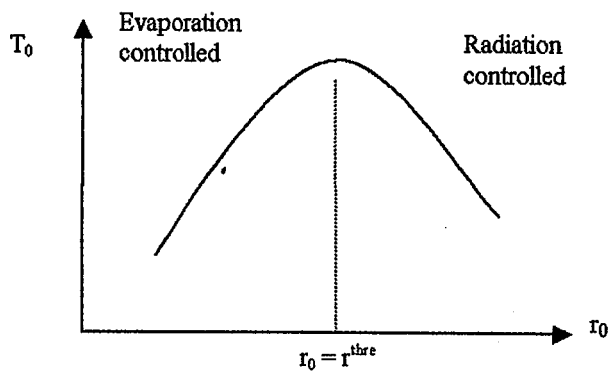

Fig. 2 Typical relationship between Surface temperature (T_0) and the Surface albedo (r_0)

The positive slope of this regression curve suggests an increase in temperature with increasing albedo until moisture is depleted and a critical metric pressure is reached. This indicates that as the surface dries up, more sensible heat becomes available to the surrounding and also reduced soil moisture increases the albedo. The lower region portion of this positive trend is supposed to be well-watered or open water bodies where potential evapo-transpiration takes place ($H \approx 0$). This portion is therefore evaporation controlled up to the peak of the curve where evaporation ceased due to depleted soil moisture. This rising part of the curve therefore means that evapo-transpiration is governing energy balance as most of the energy is used for evapo-transpiration.

At the peak of the curve where evapo-transpiration becomes zero ($\lambda E = 0$), all energy available is used for increasing the surface temperature (Daka, 1997). The value of the surface albedo (r_0), at the turning point of the curve is called the threshold value (r^{thr}). This negative trend ($r_0 > r^{thr}$) is indicative of more radiation being reflected leaving less energy for heating the surrounding in resulting decreasing temperature as the albedo increases. This portion is yielded a radiation-controlled region of the area. In SEBAL, the pixels of the surface albedo map under the region where $r_0 > r^{thr}$ are called dry pixels where as the pixel $r_0 < 0$ are called wet pixels.

3.7 Evapo-transpiration as a residual of energy balance

Actual evapo-transpiration, ET_a (mm day^{-1}), is defined as the quantity of water that evaporates from a land surface per unit area, per unit time, given the present hydro-meteorological situation. The land surface can be cropped, bare or

partially covered. The potential evapo-transpiration, ET_p (mm day^{-1}), is defined as the quantity of water that can evaporate from a land surface per unit area, per unit time, under the condition of optimum water supply. (Bastiannssen, Roerink et al.,1997)

SEBAL calculates the latent heat flux density, λE (W m^{-2}), as the residue of the surface energy balance equation, i.e. $\lambda E = Q^* - G_0 - H$.
The actual evapo-transpiration (mm day^{-1}) can be calculated from the daily-integrated latent heat flux according to (Bastiannssen, Roerink et al.,1997):

$$ET_a = 10^3 \int_0^{24} [\lambda E(t) / \lambda \rho_w] \, dt \qquad [\text{mm day}^{-1}] \qquad (3)$$

Where
λ = latent heat vaporisation [J kg^{-1}]
ρ_w = density of water [kg m^{-3}]

In the situation without water stress (potential evapo-transpiration, H=0) the surface will use all available energy ($Q^* - G_0$) for evapo-transpiration. Then potential evapo-transpiration becomes:

$$ET_p = 10^3 \int_0^{24} [\{Q^*(t) - G_0(t)\} / \lambda \rho_w] \, dt \qquad [\text{mm day}^{-1}] \qquad (4)$$

The relative evapo-transpiration can be expressed as:

$$ET_{rel} = ET_a / ET_p \qquad [-] \qquad (5)$$

The instantaneous version of this term is called the evaporative fraction:

$$\Lambda = \lambda E / [Q^* - G_0] \qquad [-] \qquad (6)$$

Shuttleworth *et al.*(1989) showed that the mid day Λ - value is almost similar to the daily value of Λ. Then the actual, potential and relative evapo-transpiration can be obtained from the instantaneous SEBAL output as:

$$ET_{rel} = \Lambda \qquad [-] \qquad (7)$$
$$ET_a = \Lambda \, ET_p \qquad [\text{mm day}^{-1}] \qquad (8)$$

To calculate the potentials value of the evapo-transpiration (ET_p), the values of G_0 and Q^* on a daily basis have to be known. In 24 hours G_0 often equals zero, so only the daily Q^* has to be calculated from instantaneous values computed. The latter can be realised by relating instantaneous to daily radiation values (Kustas et al., 1994);

$$Q^*_{24} = (1 - r_0) K^{\downarrow}_{24} - \varepsilon_0 \sigma T_{0,24}^4 + \varepsilon' \sigma T_{a,24}^4 \qquad [\text{J s}^{-1} \text{m}^{-1}] \qquad (9)$$

Where,
Q^*_{24} = average daily net radiation [J s^{-1} m^{-1}]
$K^{\downarrow}_{24}$ = average daily incoming shortwave solar radiation [J s^{-1} m^{-1}]
σ = Stefan Boltzman constant ($5.67 * 10^{-8}$) [J s^{-1} m^{-1} K^{-1}]
$T_{0,24}$ = Average daily surface temperature [K]
$T_{a,24}$ = Average daily atmospheric temperature [K]

4. Multi-spectral data and input needs

4.1 Multi-spectral data in SEBAL

Land surface fluxes vary spatially as a result of spatial heterogeneity of soil physical properties, fractional soil cover, land use, rainfall and hydrological processes. SEBAL is associated with energy balance modelling on the basis of thermal infrared measurements and all heat fluxes derived from surface radiation parameters. The SEBAL algorithm applied to this research study has been developed to solve the energy balance equation on a pixel by pixel basis (Bastiaanssen., 1995). Multi spectral images, which cover the spectral range within visible, near infrared and thermal infrared, can be used to compute the components of surface energy balance. The Landsat TM images provide this

requirement since it covers the spectral range between 0.45 μm and 12.5 μm with seven spectral windows (i.e. seven bands).

4.2 Remote sensing input needed for SEBAL operations

The physically based multi-step SEBAL needs three basic input parameters namely hemispherical surface reflectace r_0, vegetation index NDVI, and surface temperature T_0. The hemispherical surface reflectance is commonly referred as surface albedo (r_0). By inter relating these three input parameters, SEBAL computes other land surface parameters being required for estimating the components of surface energy balance.

4.3 Surface albedo (r_0)

All Landsat TM bands, except band 6, acquire shortwave radiances receiving from the atmosphere within each spectral range (spectral window). These bands acquire the reflectance properties of solar radiation of different land cover classes (when corrected for atmosphere). This can be simplified as short wave range TM bands acquire the spectral properties at top of the atmosphere.

4.4 Vegetation Index (NDVI)

Because chlorophyll (green vegetation) has a strong absorption in the TM band 3 (red) and strong reflection in the TM band 4 (near infrared), land surface spectral reflectances (r) provide information on surface vegetation conditions. Hence, Normalised Difference Vegetation Index (NDVI) is defined as below;

$$NDVI = [r(\text{infrared}) - r(\text{red})] / [r(\text{infrared}) + r(\text{red})] \quad [-] \qquad (10)$$

Spectral values of TM band 4 and 3 are needed as inputs for the determination of vegetation index.

4.5 Surface Temperature (T_0)

Band 6 of the Landsat TM data provides the spectral variations of longwave radiation receiving from the atmosphere. Since the spectral range of the TM band 6 is within the thermal infrared region, spectral values of the TM band 6 are related with the temperature variations of the different land cover classes (when corrected for atmosphere). The spectral value of TM band 6 is needed as input for the computation of surface temperature.

5. Atmospheric corrections for SEBAL inputs

5.1 Surface albedo

The amount of shortwave solar radiation reaching the land surface, $K^{\downarrow}$, depends on atmospheric absorption and scattering of short wave radiation. An explicit description of aerosol scattering can be avoided by recognising a macroscopic atmospheric perturbation on radiation transfer by means of an effective transmission coefficient, τ_{sw} in the shortwave range:

$$\tau_{sw} = K^{\downarrow} / K^{\downarrow}_{TOA} \qquad [-] \qquad (11)$$

where $K^{\downarrow}_{TOA}$ is the radiation entering the top of the atmosphere at a horizontal plane between 0.3 and 3.0 μm (i.e. shortwave radiation). A portion of the direct solar beam $K^{\downarrow}_{TOA}$ is due to Rayleigh scattering converted into the path radiance in the upper part of the atmosphere, $K^{\uparrow}_{a}$. Radiance observed by satellite sensors relate to a small field of view at the top of atmosphere and which are directional (Bastiaanssen, 1995).

A simple semi-empirical radiation transfer model proposed by Arino et al.(1992) is used for computation of r_0.

$$r_0 = (r_p - r_a) [\tau_{sw}^{"} + r_d (r_p - ra)]^{-1} \qquad [-] \qquad (12)$$

Where r_a is the atmospheric reflectance ($K_a^{\uparrow} / K^{\downarrow}_{TOA}$), and r_d is the atmospheric reflectance of diffuse radiation and $\tau_{sw}^{"}$ is the two-way atmospheric shortwave transmittance. The hemispherical surface reflectance r_0 (referred as surface albedo,) is defined as the fraction of incoming shortwave radiation at the land surface, at one particular moment, and which is reflected from land surface elements ($K^{\uparrow} / K^{\downarrow}$).

In absence of sky diffuse radiance and specularly reflected sunlight, i.e. $r_d = 0$, Eq.12 can also be shaped in a linear form (Ahern et al.,1977);

$$r_0 = (r_p - r_a)/\tau_{sw}^{"} \qquad [-] \qquad (13)$$

The relation between r_0 and r_p can be established by plotting measured surface albedo's against corresponding planetary albedo's, and fitting the data by linear regression;

$$r_0 = (1/\tau_{sw}^{"})\, r_p + (-r_a/\tau_{sw}^{"}) \qquad [-] \qquad (14)$$

Since no field measurements for r_0 are available, by using the standard values of r_0, for identified areas such as water ($r_0 \approx 0.05$), green vegetation ($r_0 \approx 0.15$), and bare soil ($r_0 \approx 0.25$), r_0 can be computed. The value of $\tau_{sw}^{"}$ was calibrated from Eq.14 using latter standard values.

5.2 Normalised difference vegetation index (NDVI)

For the NDVI, comparison has to be made between field measurements and standard calculations, in order to get an atmospheric correction. The NDVI at the top of the atmosphere can be obtained from the Eq.10. Negative NDVI values (for water bodies) shall be set at zero. Since no field measurements for NDVI are available, atmospheric correction was not established.

5.3 Surface temperature (T_0)

Surface temperature is one of the principal parameters required for the SEBAL model. It is one of the key factors in determining the exchange of energy and matter between the earth's surface and the atmosphere. The surface temperature is being calculated with the aid of TM band 6, which lies in the thermal infrared region (10.4– 12.5 μm) of the electromagnetic spectrum. The radiance of the band 6, which the satellite measures at the top of the atmosphere, has to be found with the standard calibration for Landsat TM band 6 (Roerink, 1995).

Atmospheric disturbances may have a significant effect on the outgoing narrow band longwave radiation (band 6 of Landsat TM data) which is measured at the top of the atmosphere (L_6^{TOA}). In order to convert L_6^{TOA} into the radiation emitted and reflected at the land surface ($L_6(T_0^R)$), measurements of at least two ground points must be available. Temperature values at Kirindi oya meteorological station and sea surface were available for the study.

$$L_6^{TOA\uparrow} = \{\varepsilon_0 L_6^{\uparrow} + (1-\varepsilon_0)\varepsilon_6^{'} L_6^{atm\downarrow}\}\, \tau_{lw} + L_6^{atm\uparrow} \qquad [Wm^{-2}\,\mu m^{-1}] \qquad (15)$$

Where $L_6^{atm\uparrow}$ is the up welling spectral radiance from atmospheric emission and scattering that reaches the sensor. $L_6^{atm\downarrow}$ is the down welling spectral radiance from atmospheric emission incident upon the land surface. Since the temperature value at surface incoming longwave radiation is assumed as uniform all over the image, $L_6^{atm\downarrow}$ also become a constant all over the image. τ_{lw} is the spectral atmospheric transmission. Eq.15 can be simplified as;

$$L_6^{TOA\uparrow} = (\tau_{lw})\, L_6^{sur} + L_6^{atm\uparrow} \qquad [Wm^{-2}\,\mu m^{-1}] \qquad (16)$$

Where;

$$L_6^{sur} = [\varepsilon_0 L_6^{\uparrow} + (1-\varepsilon_0)\varepsilon_6^{'} L_6^{atm\downarrow}] \qquad [Wm^{-2}\,\mu m^{-1}] \qquad (17)$$

Then an atmospheric correction procedure can be established by plotting the, $L_6^{TOA\uparrow}$ obtained from the images, and L_6^{sur} calculated from the field measurements.

By inter relating the basic parameters r_0, NDVI, and T_0, SEBAL process can be operated to solve the energy balance equation;

$$\lambda E = Q^* - G_0 - H \qquad [Wm^{-2}] \qquad (18)$$

The latent heat flux, λE is then obtained as the residue of the Eq 18.

6. Results

At the end of the SEBAL process, it provides the out put image of actual evapo-transpiration on pixel by pixel basis with mm day^{-1}. Samples of different land use / land cover types have been considered for the computation of ET_act. Graphical representations of actual evapo-transpiration (Et_act) for different land use / land cover samples are shown in

Fig.3. Et_act values (mm per day) are given, against the cumulative percentage of the number of pixels within the sample area.

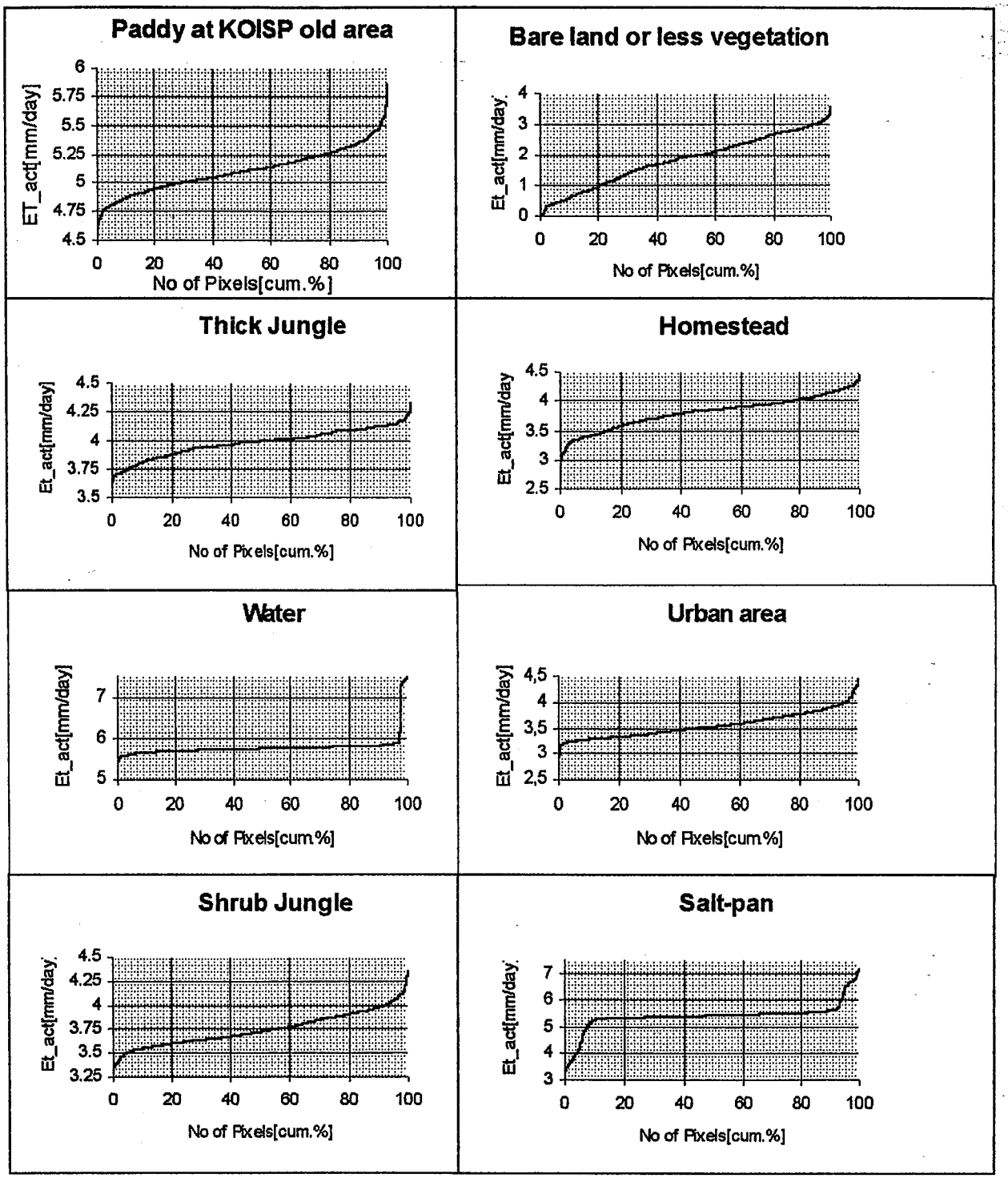

Fig.3 Actual ET values different land surface samples against cumulative percentage of pixels for the date 19th June 1995.

The values are varying within a certain range. At macro level, land use/ land cover can be categorised into different classes such as forest, grass, paddy, bare soil, water, urban, etc. and can be treated as homogeneous. Landsat TM provides the satellite images with the resolution of 30 m* 30 m pixels. At the pixel level, such land classes cannot be treated as homogeneous because of mixed vegetation, and other spatial differences. For instant, in a large reservoir, spectral properties of the water surface closer to the upstream peripheral may differ from the deeper areas due to the quality of water. In paddy fields, spectral properties may differ from area to area due to the different growing stages of paddy. Therefore any specific value of ET_act cannot be assigned for a certain land use / land cover type even though the results are on daily basis.

7. Concluding remarks

7.1 Conclusion

The results achieved in this study confirm the competence of using remote sensing data for mapping actual evapo-transpiration on different land cover / land use of the Kirindi Oya watershed. SEBAL computes the latent heat flux as the residual of the surface energy balance and thereby the evaporative fraction, which computes the actual evapo-transpiration in millimetres per day. Traditional methods compute potential ET instead of actual ET. And also such methods derive ET values for specified single crop types related to a reference crop and no facilities are available for land surfaces with mixed vegetation.
SEBAL outputs are independent from the land cover / land use. The user gets the advantage of estimating the actual water consumption using more precise values of evapo-transpiration on pixel basis (with co-ordinates). This is a challenge for the classical methods in which calculating only crop evapo-transpiration (agricultural crops) based on an identified reference crop.

7.2 Recommendations

Following recommendations can be made in order to improve the results in SEBAL level.

- Instead of taking the sea surface temperature, another point on the land surface, within the study area, shall be obtained.
- Field measurements obtained from the radiometers can be used to improve the semi-empirical relationships used to determine the SEBAL parameters.
- A relationship for NDVI at top of the atmosphere and the land surface is one example.
- Validation should be carried out at least at the regional level for the verification of the results. This will become a new project.

Reference

Arino, O., R.B. Myneni and B.J. Choudhury, 1992. Determination of land surface spectral reflectances using METEOSAT and NOAA/AVHRR shortwave channel data. Int. J. of Rem. Sens., vol 13, No. 12:2263-2287.
Ahern, F.J., D.G. Goodenough, S.C. Jain, V.R. Rao and G. Rochon 1977. Use of clear lakes as standard reflectors for atmospheric measurements, in Proc. 11th Int. Symp. On Rem. Sens. Of the Envr: 731-755.
Bastiaanssen, W.G.M., 1995, Reginalisation of surface flux densities and moisture indicators in composite terrain. A remote sensing approach under clear skies in mediterranean climates. Report 109. DLO Winand Staring Centre, Wageningen (The Netherlands).
Bastiaanssen, W.G.M., Chambouleyron, J., Menenti, M., Roerink, G. J., 1996, Relating crop water consumption to irrigation water supply by remote sensing, Water resources management 11, Kluwer Academic Publishers. Pp 445-465.
Daka. A., 1997. Land coverwise actual evapo-transpiration in western province of Zambia, MSc thesis.
Kustas, W.P., R.T. Pinker, T.J. Schmugge and K.S.Humes, 1994. Daytime net radiation estimated for a semiarid rangeland basin from remotely sensed data, Agr. And Forest Met. 71: 337-357.
Reeves, R.G., A. Anson, D. Landen, 1975. Manual of remote sensing. Volome I – Theory, instruments, and techniques. Published by the American society of photogrammetry, Verginia.
Roerink., G.J. 1995. SEBAL estimation of the aerial patterns of sensible and latent heat fluxes over the HAPEX – Sahel grid. A case study on 18 September 1992. DLO-Staring Centre, Wageningen, The Netherlands.